Invertebrate Zoology, 2025, 22(4): 595–613

New data on early astogeny and microstructure of cystid in *Patinella verrucaria* (Bryozoa: Cyclostomatida)

A.E. Vakhrushev[1,2], E.N. Temereva[2,*]

[1] *Invertebrate Zoology Department, Lomonosov Moscow State University, Leninskie Gory 1-12, Moscow 119234 Russia.*
[2] *Evolutionary Biology Department, Lomonosov Moscow State University, Leninskie Gory 1-12, Moscow 119234 Russia.*
**Corresponding author*
Elena Temereva: temereva@mail.ru ORCID https://orcid.org/0000-0001-7791-0553
Alexey Vakhrushev: a.e.vakhr@gmail.com ORCID https://orcid.org/0009-0003-9622-9212

ABSTRACT: Cyclostomatida is one of two groups of recent bryozoans with a skeleton of calcium carbonate. Unlike Cheilostomatida, the skeleton of cyclostome bryozoans has a small set of characters that can be used for identification and phylogenetic analysis. In this study, we used computed microtomography (mCT) and scanning electron microscopy (SEM) to deepen our understanding of the early stages of development and microstructural characteristics of representatives of the Lichenoporidae family using *Patinella verrucaria* as an example. The outer wall of the colony has a granular microstructure and is covered with a cuticle. In the inner colony walls, we registered three zones composed of only two fabrics: the accretion zone (with a granular fabric), the transition zone, and the zone of foliaceous crystallites (both with a foliated fabric). The inner wall of the colony has numerous outgrowths, or pustules, arranged in rows along the growing edge of the colony. They reach their maximum size at a certain distance from the colony centre and can be involved in the transport of materials within the colony. The process of skeletal formation in *P. verrucaria* is similar to that of other cyclostome bryozoans and resembles the process of biomineralization observed in Mollusca. Microscopic skeletal features are important identification characters at both the genus and species levels and also can be used to identify growth zones within a colony. Our data on the skeletal microstructure of the alveoli suggest that they are kenozooids. The study of young colony development using light microscopy and, for the first time, mCT confirmed two options of colony development relative to the growth direction of the first zooid: right- and left-directional scenarios. This phenomenon exemplifies the enantiomorphic colonies recorded in recent cyclostomes. The two mirror types of early colony development have a ratio of 470 (right):394 (left), suggesting either a genetic determination of growth or a significant influence of the physical characteristics of the substrate on colony development.
How to cite this article: Vakhrushev A.E., Temereva E.N. 2025. New data on early astogeny and microstructure of cystid in *Patinella verrucaria* (Bryozoa: Cyclostomata) // Invert. Zool. Vol.22. No.4. P.595–613. doi: 10.15298/invertzool.22.4.06

KEY WORDS: colony development, computer microtomography, scanning electron microscopy, enantiomorphy, symmetry features, Lichenoporidae, White Sea.

Новые данные раннего развития и микроструктуры цистида *Patinella verrucaria* (Bryozoa: Cyclostomatida)

А.Е. Вахрушев[1,2], Е.Н. Темерева[2,*]

[1] Кафедра зоологии беспозвоночных, Московский государственный университет имени М.В. Ломоносова, Ленинские горы 1-12, Москва, 119234 Россия.
[2] Кафедра биологической эволюции, Московский государственный университет имени М.В. Ломоносова, Ленинские горы 1-12, Москва, 119234 Россия.
** Ответственный за переписку: temereva@mail.ru*

РЕЗЮМЕ: Циклостоматы — одна из двух групп современных мшанок со скелетом из карбоната кальция. В отличие от хейлостомных мшанок, скелет циклостомат обладает небольшим набором признаков, которые могут быть использованы для идентификации и филогенетического анализа. В настоящем исследовании мы с помощью методов компьютерной микротомографии (мКТ) и сканирующей электронной микроскопии (СЭМ) расширяем данные по раннему развитию и микроструктуре для семейства Lichenoporidae на примере вида *Patinella verrucaria*. Внешняя стенка обладает микроструктурой гранулярного типа и покрыта кутикулой. Мы выявили три зоны во внутренних стенках колонии: зона заложения кристаллов (имеющая микроструктурой гранулярного типа), переходная зона и зона черепитчатых кристаллов (обе обладают микроструктурой листовидного типа). Внутренняя стенка колонии несет многочисленные выросты, или пустулы, расположенные рядами вдоль растущего края колонии. Они достигают максимальной высоты на некотором удалении от центра колонии и могут быть вовлечены в транспорт веществ по колонии. Процесс формирования скелета *P. verrucaria* аналогичен таковому у других циклостомат и схож с процессом биоминерализации у моллюсков. Особенности микроструктуры скелета являются важными определительными признаками как на родовом, так и на видовом уровнях, а также могут быть использованы для идентификации зон роста в пределах колонии. Наши данные о микроструктуре скелета альвеол позволяют предположить, что последние являются кенозооидами. Изучение раннего развития колонии с использованием световой микроскопии и, впервые, компьютерной микротомографии подтвердило наличие двух вариантов развития колонии относительно направления роста первого зооида: право-направленный и лево-направленный сценарии. Этот феномен является примером энантиоморфии на уровне колоний, зарегистрированным у современной циклостомной мшанки. Два зеркальных типа раннего развития колонии имеют соотношение 470 (правых):394 (левых), что позволяет предположить либо наличие генетического предопределения роста колонии, либо указывает на значительное влияние физических характеристик субстрата на раннее развитие колонии.
Как цитировать эту статью: Vakhrushev A.E., Temereva E.N. 2025. New data on early astogeny and microstructure of cystid in *Patinella verrucaria* (Bryozoa: Cyclostomata) // Invert. Zool. Vol.22. No.4. P.595–613. doi: 10.15298/invertzool.22.4.06

КЛЮЧЕВЫЕ СЛОВА: развитие колонии, компьютерная микротомография, сканирующая электронная микроскопия, энантиоморфия, особенности симметрии, Lichenoporidae, Белое море.

Introduction

Bryozoa is a phylum of Metazoa that is represented only by colonial organisms. Bryozoan colony consists of modules, zooids. The body wall of each zooid has a skeleton, either purely organic or calcareous. Among Bryozoa, two of the three classes, Gymnolaemata and Stenolaemata, possess skeletons composed of calcium carbonate. These classes are well known in the fossil record (Taylor, 1994; McKinney, 1998; Ernst *et al.*, 2015; Ma *et al.*, 2015; Pruss *et al.*, 2022). Stenolaemate bryozoans are the oldest within phylum and have been known since the Cambrian or Ordovician (Ma *et al.*, 2015; Pruss *et al.*, 2022) and have been abundant throughout the Phanerozoic (Ernst, 2017, 2020). However, recent stenolaemate bryozoans are represented by only one exclusively marine order, Cyclostomatida, and were abundant throughout the Phanerozoic (Ernst, 2017, 2020).

All cyclostome bryozoans are marine and, unlike cheilostomes, exhibit a limited number of skeletal features. The zooidal skeleton of cyclostomes is usually tubular in shape and terminates in a distal aperture through which the tentacle crown emerges for feeding. Soft tissue anatomy is known for a small number of species (Borg, 1926; Nielsen, 1970; Nielsen, Pedersen, 1979; Boardman *et al.*, 1992; Boardman, 1998; Schwaha *et al.*, 2018; Temereva, Kosevich, 2018; Nielsen *et al.*, 2019; Worsaae *et al.*, 2020; Tamberg *et al.*, 2021, 2022), and even fewer molecular sequence data are available (Waeschenbach *et al.*, 2009; Taylor *et al.*, 2015, 2021). Hence, the most important morphological characters in the taxonomy of Cyclostomatida are related to skeletal features: skeletal structure, budding pattern, colony shape, arrangement of autozooidal apertures, and the shape of the gonozooid (or brood chamber) and its opening, the ooeciostome. Furthermore, since many representatives of Stenolaemata are extinct, these characters are the only ones that can be used in taxonomic studies. Skeletal features have long been used in phylogenetic studies and taxonomic identification (Brood, 1976; Schäfer, 1991; Viskova, 1992; Taylor, Weedon, 2000). However, they do not always reflect the true relationships between groups (Waeschenbach *et al.*, 2009; Taylor *et al.*, 2021) due to their high phenotypic plasticity and convergent evolution (Hinds, 1975, Blake, 1980; Waeschenbach *et al.*, 2009).

Scanning electron microscopy (SEM) allowed us to examine the skeleton from a new angle. It has been shown that, like in other animal groups with calcium carbonate skeleton, such as molluscs and brachiopods, the mineralized structures of bryozoans are secreted by the epithelium and are built from large numbers of small crystallites (Tavener-Smith, Williams, 1972; Weedon, Taylor, 1995). The secretion of mineral components occurs after the formation of an organic layer, the so-called cuticle or periostracum. The crystallites of cyclostomes have various crystallographic characteristics, which are used to determine the microstructure of fabrics (Weedon, Taylor, 1997; Taylor, Weedon, 2000), and the combination of different fabrics is called the fabric suit. Both fabrics and fabric suits can be used for phylogenetic analyses (Taylor, Weedon, 2000; Waeschenbach *et al.*, 2009; Taylor *et al.*, 2021). In addition, these microstructural features can provide insight into skeleton formation (Taylor, Jones, 1993; Taylor *et al.*, 1995) and adaptations to maintain colony strength (Weedon, Taylor, 1997). Despite the obvious benefits of using microstructural features for understanding the colony structure and function, their use in phylogenetic analysis is difficult and is considered to be highly homoplastic (Taylor, Weedon, 2000).

Recently, structural features of early stages and early colony development of cyclostomes have been investigated to better understand their phylogeny (Taylor *et al.*, 2015). Cyclostome colonies arise from ciliated, free-swimming larvae that metamorphose into a calcified, hemispherical protoecium soon after settlement (Nielsen, 1970; Nielsen *et al.*, 2019). The protoecium extends a calcified tube, develops a tentaculate polypide, and becomes a functional ancestrula (Nielsen, 1970). Although features of the protoecium and early astogeny are potentially taxonomically significant (Taylor *et al.*, 2015), these characteristics have been studied in a few representatives of the order (Borg, 1926; Taylor *et al.*, 2015; Batson *et al.*, 2019). In addition to the taxonomic value, early astogeny exhibits some unusual phenomena. Thus, Harmer (1896) discovered that colonies of *Patinella verrucaria* (=*Lichenopora veruucaria*) can develop in two different ways. The first way is right-handed: the first zooid of the colony grows to the right and the second zooid grows to the left. The second

way is left-handed: the first zooid of the colony grows to the left and the second zooid grows to the right (Harmer, 1896). In addition to describing these developmental scenarios, Harmer showed that out of 16 randomly selected young colonies, 8 developed according to the right-handed way and 8 according to the left-handed way. Right- and left-handed colonies have been reported for some extant and extinct bryozoans (e.g., McKinney, Burdick, 2001), and such feature represents the phenomenon of enantiomorphy (Viskova, 2013, 2014). However, additional data on the possible causes of enantiomorphic development and its regulation, as well as on the potential applications of this phenomenon in taxonomy, are currently almost absent. Additionally, new techniques such as computed microtomography have never been applied to the study early astogeny in cyclostomes.

Studies of the fine structure, growth, and development of the skeleton in cyclostomes are essential for understanding their phylogenetic relationships. In addition, data on skeletal microstructure and the use of new methods to study colony development can improve our understanding of skeletal formation and the importance of symmetry features in early astogeny in lichenoporids. The aim of this study was to use new methods (mCT, SEM) for further examination and re-evaluation data on the structure, growth and development of the mineral skeleton of *Patinella verrucaria*, a member of the Lichenoporidae family (suborder Rectangulata).

Material and methods

Sampling

All samples were collected in June-August in 2023–2025 in the vicinity of MSU White Sea Biological Station by SCUBA diving. Species were identified according to Gostylovskaya (1978). For light microscopy, colonies were photographed in the laboratory using Leica M165C (Leica, Germany) stereomicroscope equipped with Leica DFC420 digital camera.

Scanning electron microscopy (SEM) and computer micro tomography (mCT)

For SEM and mCT studies, collected colonies were fixed in 96% ethanol and stored in it. Fixed colonies were exposed in 15% commercial bleach solution for 48–72 hours at room temperature. It was necessary for removing soft tissues (e.g., cuticle). After that, colonies were washed in distilled water. For SEM studies, 17 colonies were dehydrated in pure ethanol, transferred to a mixture of ethanol and acetone (1:1) followed with pure acetone, and then colonies were critical point dried. Colonies and broken or sawn parts of colonies were attached on double-sided tape to metal stubs and coated with platinum-palladium. Specimens were examined with JSM-6380 scanning electron microscope at an accelerating voltage of 20 kV. For mCT, 6 colonies were dehydrated in pure ethanol, transferred to a mixture of ethanol and acetone (1:1) followed with pure acetone, and then colonies were air-dried, attached on micropipette tip with glue and studied with SkyScan 1272 (Bruker Corporation) microtomograph. For all specimens, the source current was 145 μA, the source voltage was 50 or 55 kV, isotropic voxel size was 1.8, 2.1, and 3.3 μm. Exposure time was 1425 ms, an angular increment of 0.2° between projections. For all specimens, the frame averaging was ON. Camera to source distance in all cases was 274 mm, object to source distance was 33, 34, 38, and 61 mm. The analysis of the obtained 3D images was performed using the CTvox.

Observation of early astogeny

Early astogeny studying was performed with mCT (6 colonies) and light microscopy (858 live colonies). In both cases, identification of development types was carried out when viewed from above in proximal-distal growth direction of the first zooid (from ancestrula to the growing edge of the colony). For light microscopy, colonies were counted and photographed in the laboratory using a Leica M165C (Leica, Germany) stereomicroscope equipped with a Leica DFC420 digital camera.

Terminology

In this paper, we follow the terminology of Taylor and coauthors (Taylor *et al.*, 1995).

Results

General morphology of colonies

Patinella verrucaria has white, disk-shaped, encrusting colonies with a basal wall that is raised above the substrate at the edges (Fig. 1A). The size of studied colonies varied greatly. The maximum diameter of mature colonies reached 1–2 mm. Autozooids are elongated and tubular with circular apertures 100–200 μm in diameter. The upper apertural margin forms 1 to 3 apertural spines, or "pseudolunaria" (Fig. 1B, C), their length is about 30–35 μm. Autozooids are arranged in irregular rows extending from the centre to the edge of the colony. Alveoli are located between the autozooids; they are 100–120 μm in diameter and are devoid of polypide. In the central part of the colony, there is a brood chamber with one or more ooeciostomes (200–250 μm in diameter) (Fig. 1D).

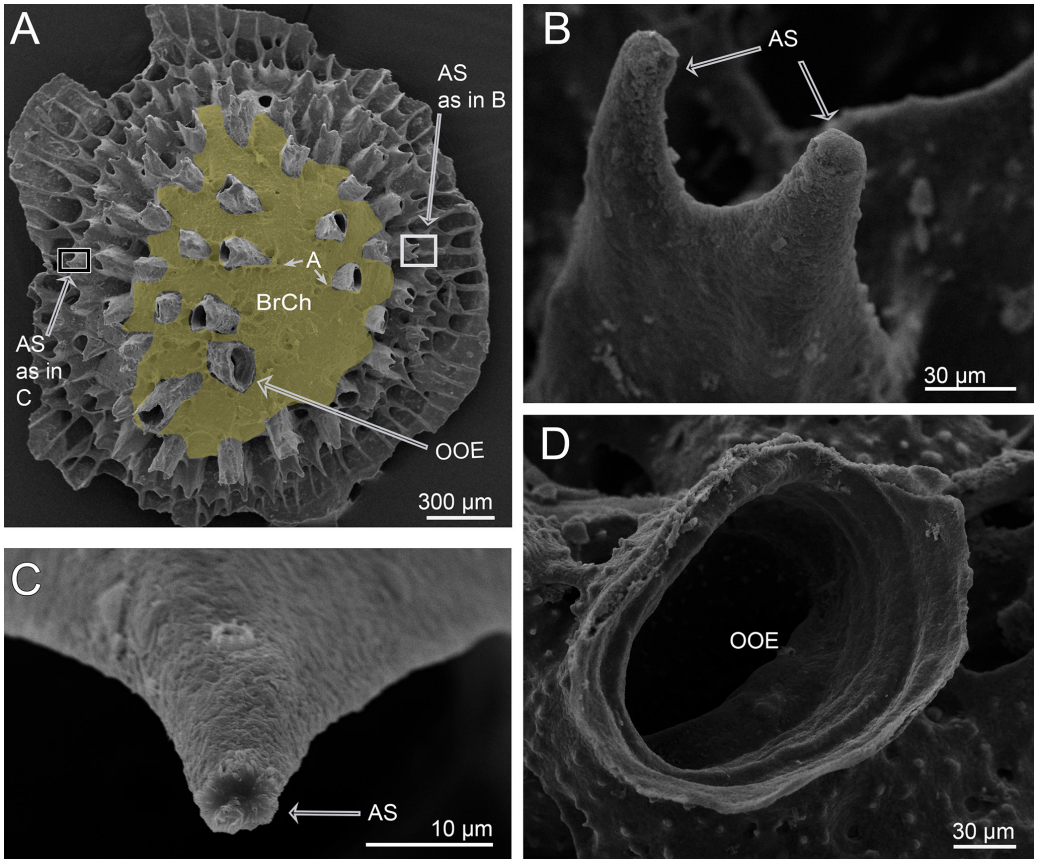

Fig. 1. General view and some features of the *Patinella verrucaria* (SEM). A — general view of the mature colony with brood chamber, which borders are shown in light green, and one ooeciostome; B — two apertural spines (as in a white square on A); C — one aperture spine (as in a square with a white-black border on A); D — ooeciostome.
Abbreviations: AS — apertural spines; BrCh — brood chamber; OOE — ooeciostome.

Features of early astogeny

Soon after larva settles, the first skeletal structure, the protooecium, forms. From it, the first zooid (Z1) starts growing parallel to the substrate. On its basal side facing the substrate, the second zooid (Z2) and the third zooid (Z3) bud off. Z2 forms slightly earlier than Z3 and on transverse tomographic sections looks like a larger outgrowth on the basal side. As Z1 increases in length, its distal part deviates from its original axis. At the same time, Z2 and Z3 grow in specific directions. The relative growth direction of these three zooids determines early stages of the colony astogeny according to one of two scenarios (they are summarized in Fig. 2A. B).

Right-handed colonies. According to the right-handed scenario (Fig. 3), Z1 bends to the right of the original axis, while Z2 located to the left of the original growth axis of the first zooid, turns to the left, and Z3, located at to the right of the original growth axis of the first zooid, grows straight along the original axis of Z1. We registered 470 right-handed colonies.

Left-handed colonies. According to the left-handed scenario (Fig. 4), Z1 bends to the left of the original axis, while Z2, located at the right side of the original growth axis of the first zooid, turns to the right, and Z3, located at the left side of the original growth axis of the first zooid, grows straight along the original axis of Z1. We found 394 left-handed colonies.

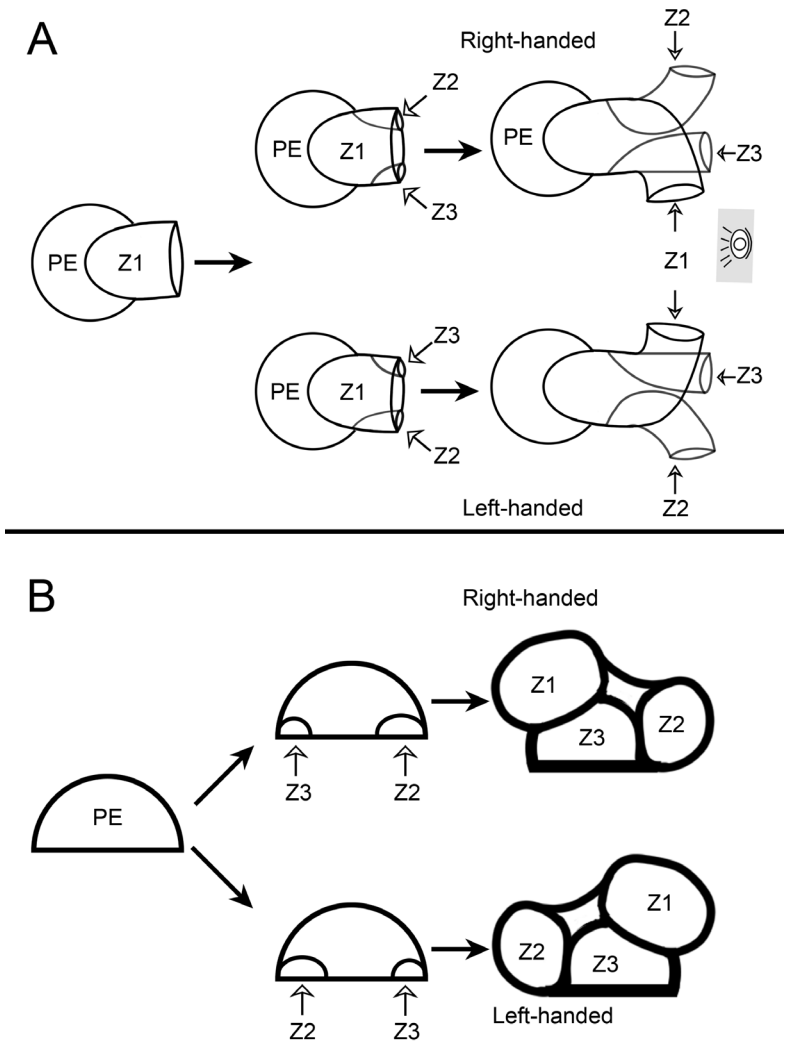

Fig. 2. Schemes of two scenarios of *Patinella verrucaria* early astogeny. A — view from the top; B — transverse sections of colony viewed from the apertures (as eye location in A). The stages on A correspond to the stages on B.
Abbreviations: PE — protoecium; Z1 — first zooid of the colony; Z2 — zooid developing mirrorable to the first zooid of the colony; Z3 — axial zooid.

In both cases, new zooids bud off. Later on, after growing parallel to the substrate, all zooids bend upwards so that the apertures are angled to the substrate surface.

Most colonies were found on red algae common in the White Sea: *Porphyra* sp., *Ptylota plumosa*, *Phycodrys rubens*, *Odonthalia dentata*, and *Palmaria palmata*. It is worth noting that left-sided and right-sided colonies were found on both sides of the algae thallus.

Skeletal microstructure

Basal wall

The basal wall is the exterior wall the lichenoporid colony. Two sides of the basal wall can be recognized: the outer side, covered with cuticle, is attached to the substrate, and the inner side is visible at the growing edge of the colony.

After bleaching, the circular stripes are clearly visible on the outer side of the basal wall (Fig. 5A, B). Their width is similar and is about 2–4

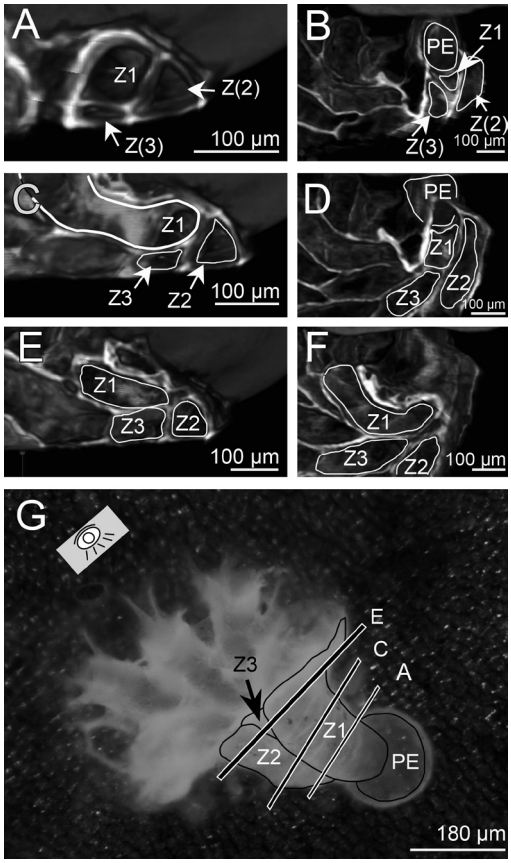

Fig. 3. Right-handed early development of the *Patinella verrucaria*. A, C, E — transverse mCT sections viewed from the growing edge (shown with the eye on G), approximate cut levels are shown on G; B, D, F — longitudinal mCT sections, viewed from above; G — general view of the right-handed colony; light microscopy.
Abbreviations: PE — protoecium; Z1 — first zooid of the colony; Z(2,3) — established zooids; Z2 — zooid developing mirroring the first zooid of the colony; Z3 — axial zooid.

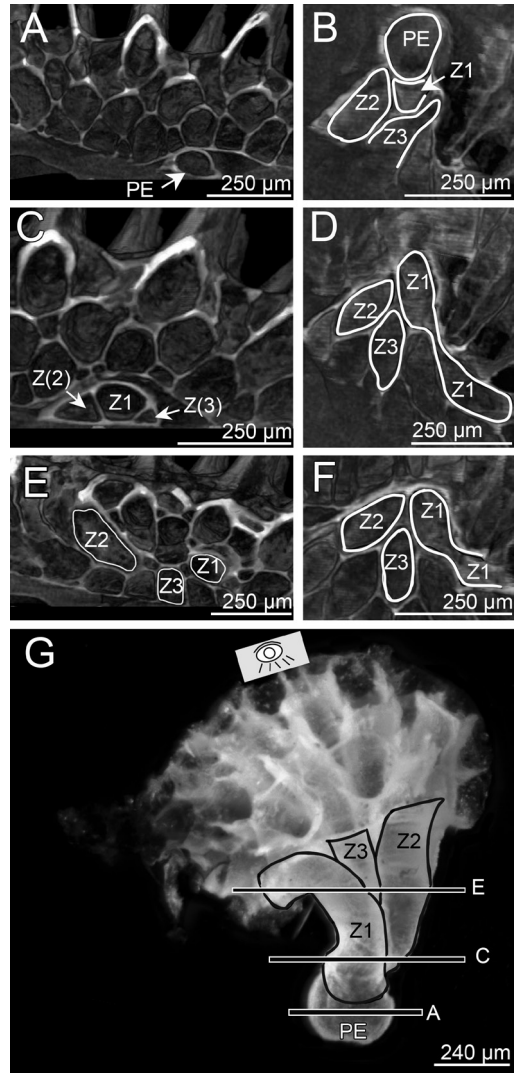

Fig. 4. Left-handed early development of the *Patinella verrucaria*. A–F and G — different colonies; A, C, E — transverse mCT sections viewed from the growing edge (shown with the eye in G), approximate cut levels are shown on G; B, D, F — longitudinal mCT sections, viewed from above; G — general view of another left-handed colony; light microscopy.
Abbreviations: PE — protoecium; Z1 — first zooid of the colony; Z(2,3) — established zooids; Z2 — zooid developing mirrorily to the first zooid of the colony; Z3 — axial zooid.

µm. Irregularly arranged crystallites of the outer side of the basal wall have a variable shape and size (Fig. 5C, D), and their length ranges from 0.3 to 1.5 µm.

The inner side of the basal wall has a pronounced zonation. Based on the structure of the crystallites, three zones can be recognized: crystallites accretion zone (composed of a granular fabric), transition and imbricated zones (both composed of a foliated fabric) (Fig. 6A). The zone of crystallites accretion (Fig. 6B) is a narrow strip (0–5 µm in width) occupying the most distal edge of the colony. The irregularly arranged crystallites have a granular shape with a diameter of 0.5–1 µm (Fig. 6B). The next zone is the transition zone (Fig. 6C) starting at a distance of 5–8 µm from the colony edge. Crystallite

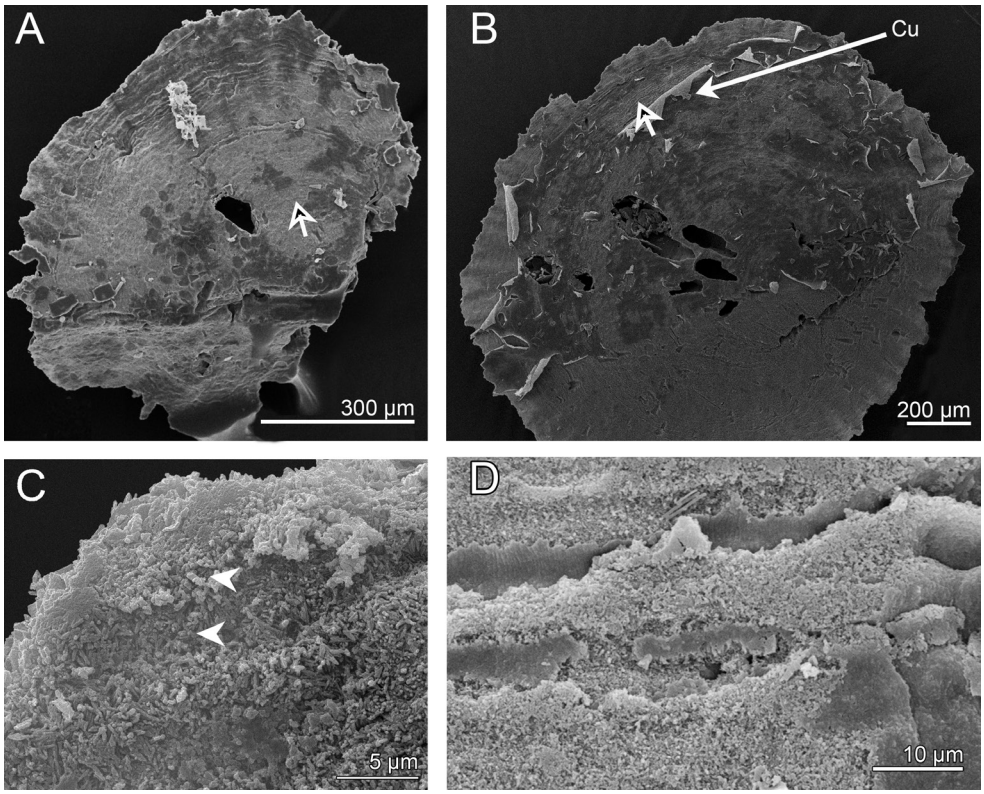

Fig. 5. Outer basal wall of the colony of the *Patinella verrucaria* (SEM). A, B — general view of the outer basal wall; A — basal wall cleaned of cuticle; B — basal wall with cuticle; C — granular crystallites of the outer basal wall on the edge of the colony; D — granular crystallites of the outer basal wall near centre of the colony.
Abbreviations: Cu — cuticle; arrows — stripes, which corresponds to the growth of the colony; arrowheads — granular crystallites.

growth occurs in the transition zone, the largest of them reach 3–4 µm in length (Fig. 6C). Despite the lack of a regular structure, separate crystallites become more foliated with an obtuse angle directed towards the growing edge of the colony (Fig. 5C). In the imbricated zone (Fig. 6D), which begins at a distance of 8–12 µm from the colony edge, crystallites eventually become foliated and has an angle of about 120 degrees at the distally faced edge of each crystallite. The foliated crystallites clearly show boundaries of the deposition of new layers, the size of this stripes ranges from 0.1 to 0.45 µm (Fig. 6E, F). Crystallites located close to the colony centre are piled on their tops located closer to the colony edge, thus forming an imbricated structure. Due such arrangement of the crystallites, their full size is difficult to measure, but their free part can reach 13 µm in length and 17 µm in width.

It should be emphasized that the described fabric suit is the most complete variation. Usually, a view from the inner side of the basal wall does not allow one to observe the zone of crystallite accretion (6E, F).

Interzooidal walls. The secretion of interzooidal walls begins directly at the growing colony edge or at some distance from it (Fig. 7A). Formation occurs in the form of septa growing upward from the basal wall (Fig. 7A, B). The youngest crystallites, which form septa near the growing edge and, at later stages, are located in the most central part of the young interzooidal wall, have a polygonal shape; their length and width are 0.5–1 µm (Fig. 7C). In shape, size, and location, these crystallites correspond to the crystallites located directly at the growing edge and on the outer side of the basal wall. Towards the centre of the colony, the height and

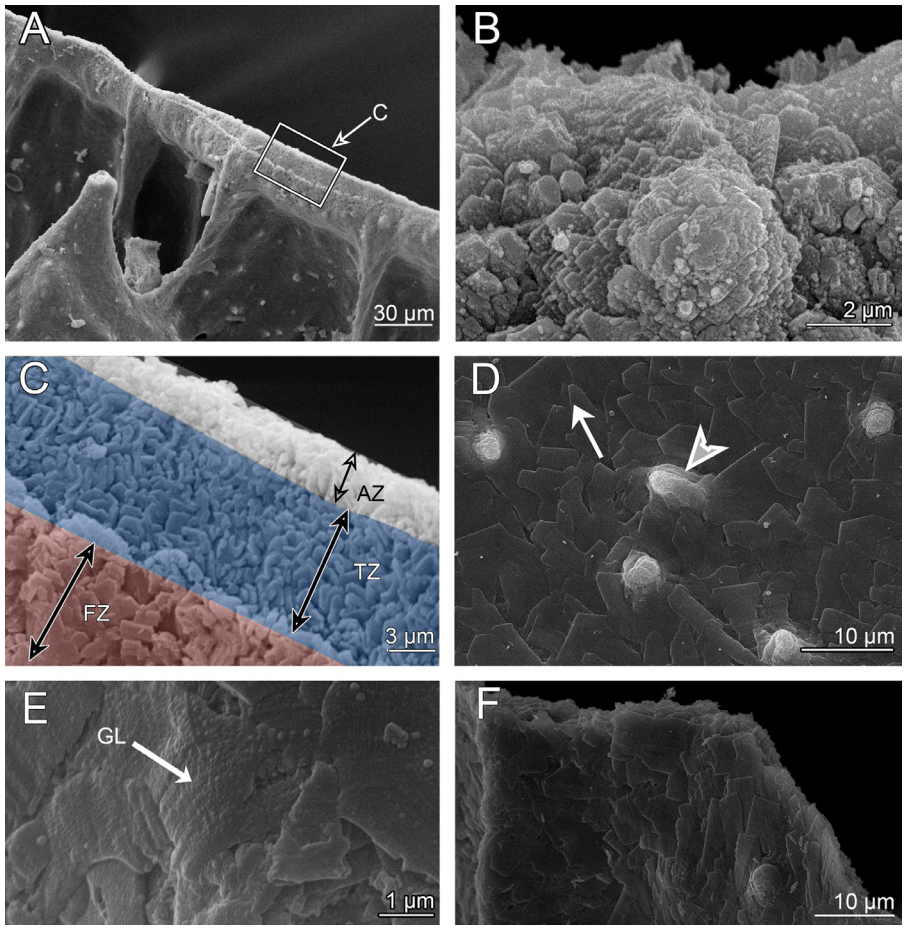

Fig. 6. Inner basal wall of the *Patinella verrucaria* (SEM). A — general view of the growing edge; B — accretion (granular) zone; C — transition zone; D — foliated zone with young pustules (white arrow — the crystallite growth direction); E — crystallites from foliated zone, note growing lines (GL); F — the edge of the colony without transition and accretion zones (they have been broken off or turned to the basal side). Abbreviations: AZ — accretion zone; FZ — foliated zone; GL — growing lines of the crystallites; Pu — pustules; TZ — transition zone; grey concaved arrowhead here and further — pustules.

width of the septa increase, and the structure of crystallites also changes. About 20 µm after the beginning of the septum, crystallites become less multifaceted, usually acquiring the shape of quadro- or hexagonal plates (Fig. 7D). Further towards to the colony center, crystallites become foliated with an angle of 120 degrees at the distal growing edge (Fig. 7E). An imbricated structure also forms (Fig. 7E).

At fracture, fully formed interzooidal walls can be characterized as symmetrical relative to the wall centre (Fig. 7F). In the centre, irregularly arranged granular crystallites is located. They are usually small, less than 1 µm in size, cuboidal or rectangular in shape. Laterally from them, there are larger crystallites, up to 2 µm long. They have the shape of a parallelepiped with triangular edges. At the edges and lateral sides of the interzooidal walls, the crystallites become more and more foliated, overlapping each other and forming an ordered, imbricated structure. Further, in the depth of the zooid or alveoli, crystallites become larger, their distal edges become angular, and imbricated structure is fully formed.

Interzooidal pores. Pores penetrate interzooidal walls and connect adjacent autozooids, they are also present between autozooids and

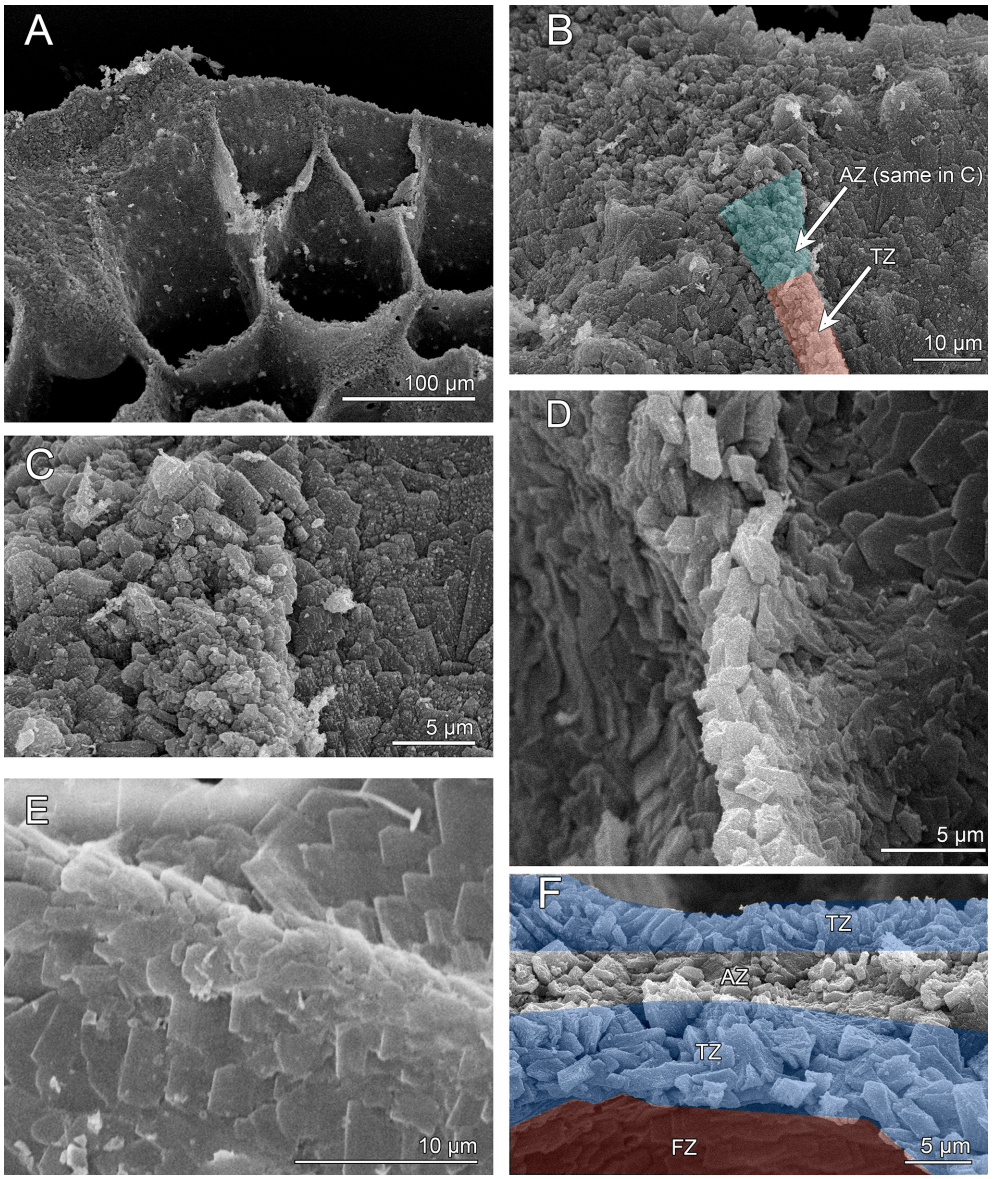

Fig. 7. Interzooidal walls of the *Patinella verrucaria* (SEM). A — general view of the growing edge with young septa (interzooidal walls); B — general view of the septa laid by granular crystallites; C — granular crystallites of the young septa; D — four-sided or hexagonal crystallites in the interzooidal wall; E — foliaceous crystallites in the interzooidal wall; F — portion of the interzooidal wall.
Abbreviations: AZ — accretion zone; FZ — foliated zone; TZ — transition zone.

alveoli, as well as between autozooids and the roof of brood chamber. In *P. verrucaria*, the pore diameter varies from 5 to 7 µm (Fig. 8A). The crystallites bordering the pores usually possess several centripetally arranged smooth spines reaching 0.5–2 µm in length. Sometimes, the spines have a distal bifurcation. Since the interzooidal wall itself consists of several layers of crystallites, the spines are also arranged in several layers.

Apertural spines. Apertural spines are outgrowths of the upper apertural margin of a mature

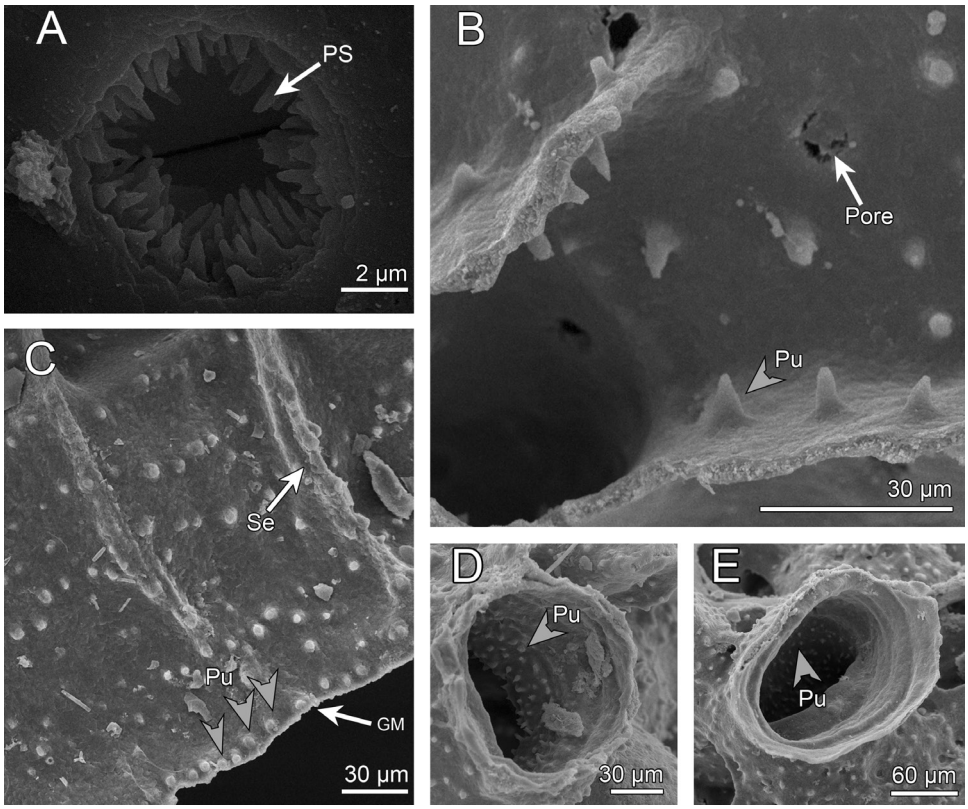

Fig. 8. Microsculpture features of the *Patinella verrucaria* (SEM). A — interzooidal pore with pore spines; B — pustulose interzooidal walls; C — growing margin of the colony with young pustules; D — ooeciostome with high-lying pustules; E — ooeciostome with low-lying pustules.
Abbreviations: GM — growing margin; Pore — interzooidal pore; Pu — pustules; PS — pore spines; Se — septa; grey concaved arrowheads — pustules.

autozooid (Fig. 1B, C); in *P. verrucaria*, there are 1–3 apertural spines per autozooid. They are arranged parallel to zooid axis and reach 40 µm in length. When there is a single apertural spine, it is located at the midsagittal plane of the autozooid and bends slightly upward. When two apertural spines present, they are located slightly apart from the midsagittal plane of the autozooid and diverge from each other, forming an acute angle of about 30 degrees. In this case, the diameter of the apertural spines in this case reaches 20 µm. When there are three apertural spines, the central one is located at the midsagittal plane of the autozooid.

Pustules. In addition to the usual imbricated crystallite structure, *P. verrucaria* has pustules (or small mural spines), which are needle-like outgrowths directed perpendicular to the zooidal walls (Fig. 8B). Pustules are located on the border of the transitional and imbricated zones, often in short rows of 2, 3 or more (Fig. 8C). Towards the colony centre, the size of the pustules gradually increases, reaching 10–12 µm in height (Fig. 8B). Besides the growing edge of the colony, the pustules are also numerous and have the same linear dimensions on all colony walls: the inner basal, interzooidal, outer and inner walls of the brood chamber. It should be noted that the colonies with different numbers of ooeciostomes display differences in the location of the pustules. If there is one ooeciostome in the colony, pustules are located close to its aperture at a distance of about 30 µm, but if there are two or more ooeciostomes, they are situated deeper, at a distance of about 100 µm from its aperture (Fig. 8D, E).

Discussion

Asymmetry in the colony development

Our data confirm the existence of two scenarios of early colony development in *P. verrucaria*, resulting in the formation of right- and left-handed colonies. These results are in good agreement with observations of Harmer (1896), who described this phenomenon. Right- and left-handed spiral and reticulated colonies were described for several extinct Stenolaemate bryozoans and unknown for recent cyclostomatids. For example, well known right-handed and left-handed reticulated colonies of the Palaeozoic genus *Archimedes* Owen, 1842, *Terebellaria ramossissima* d'Orbigny, 1852 with straight dichotomizing branches represented by descending three-dimensional spiral, *etc.* (Viskova, 2013, 2014). These findings are examples of enantiomorphy in bryozoans, which can be either zooidal or colonial (reviewed in Viskova, 2013, 2014). Enantiomorphy, or chirality, is a special type of asymmetry when an object does not superpose on its mirror image; it is also found in other metazoan phyla, and the most striking examples are the dextral/sinistral shell of snails (e.g., Freeman, Lundelius, 1982; Gould *et al.*, 1985) and the dextral/sinistral spiral tube of polychaetes of the family Spirorbinae (Palmer, 2009). We believe that right- and left-handed colony development in *P. verrucaria* belongs to this category, i.e., is an example of enantiomorphic colonies recorded in the recent cyclostomes.

However, asymmetrical forms have evolved many times among higher Metazoans (Palmer, 2009). Prominently asymmetrical forms can be classified as follows: fixed asymmetry (right or left/dextral or sinistral forms) and antisymmetry, or random asymmetry (the ratio of right and left forms is 1:1) (Palmer, 1996). Fixed asymmetry is thought to be genetically determined and is implemented mainly during the larval stage. Antisymmetry occurs due to external factors and is realized mostly in the post-larval period (Palmer, 1996, 2009). Well-known examples of random asymmetry are enlargement of either right or left claw of American lobsters (Govind, 1989) and random eye-side asymmetry in two of the three most ancient extant lineages of flounders (Palmer, 2009). In contrast to antisymmetry, fixed asymmetry is genetically determined. Fixed asymmetry has been observed in various animal groups. For instance, the human heart is located on the left side of the chest; in narwhals, the tusk develops from the left incisor; and in echinoderms, the right mesocoel is reduced. The mechanism of left-right axis determination (and thus left-right asymmetry) is similar in many animals. In the development of the lancelet *Amphioxus* or the tunicate *Halocynthia*, echinoderms such as sea urchins or protostomes such as snails, and even *Hydra*, the Nodal-factor plays an important role in the formation of the left-right axis (Blum, Ott, 2018).

As for bryozoans, there are several priority variants of young colony astogeny in *Cribrilina annulata*, although many more possible options exist (Yagunova, 2005). Such priority can be explained by two factors: (1) the specific selection of a favourable location on the substrate by the larva (external influence), and (2) morphogenetic determinism (internal influence). Nevertheless, it is likely that both of these factors influence colony development. The initial stages of bryozoan astogeny seem to be similar in different classes, indicating the fundamental similarity of the processes of their early development (Medd, 1966; Yagunova, 2005).

According to our data, the ratio of right- and left-handed colonies (470 and 394, respectively) of *P. verrucaria* suggests that this case belongs to random symmetry category and thus can be determined by both external factors and genetic basis.

External factors — substrate effects

The mechanical and chemical characteristics of the substrate are important factors for larval settlement and different stages of astogenesis (Roberts *et al.*, 1991; McKinney, McKinney, 1993; Denley *et al.*, 2014; Snijder, 2024). The chemical impact of substrate is caused by exometabolites of both the substrate itself and the bacteria living on it. Unfortunately, such data are almost absent for collected species of red algae. However, in the case of *P. verrucaria,* the substrate effect is less likely due to the presence of colonies of this species on various substrates, such as red algae, brown algae, and stones (Gostilovskaya, 1978; Demidova *et al.*, 2025). As for the mechanical effect of the substrate, its relief could prevent the bud formation on one side of the first zooid (Z1) of the colony. Thus, on its right (or left) side, the second zooid (Z2) forms earlier than the third zooid (Z3) and influences the growth direction of Z1 to grow in the opposite direction, setting a natural spatial limitation for growth in the other

direction. However, our observations failed to reveal any evident mechanical impediments to the formation of new zooids.

Genetical determination

The uneven ratio of dextral and sinistral (470:394) colonies of *P. verrucaria* suggest a genetic predetermination of their formation. With the gradual predominance of one of these polymorphic variants, there may be a shift in the proportion of dextral colonies. If Z2 becomes fertile, the transmission of a specific developmental variant may occur. Interestingly, Harmer (1896) claimed that in both right- and left-handed colonies, Z2 becomes fertile, and a brood chamber develops based on its soft tissues. This statement is crucial to understanding the inheritance of dextrality/sinistrality. Further research is needed to clarify how exactly the soft tissues of the brood chamber are formed, as well as to reveal the determinism/non-determinism of development according to one of the scenarios. Detection of similar developmental features in other representatives of this family will clarify the cause of this phenomenon. Moreover, a deeper understanding of the early astogeny of cyclostome bryozoans will be useful in phylogenetic research.

Thus, the discovery made by Harmer (1896) and confirmed by us is a unique feature of the development of recent cyclostomates; we regard it as a colonial enantiomorphy. This feature of early astogeny may fall under the phenomenon of enantiomorphy. The importance and causes of this feature remain to be determined. Moreover, this developmental feature can be useful for understanding the colony-substrate relationships, such as the substrate influence on colony development.

Skeletal microstructure

The formation of the skeletal structure in *P. verrucaria* begins with the deposition of wedge-shaped crystallites on the cuticle or on existing skeletal structures. These crystallites form a granular fabric, which is associated with the growth zone of *P. verrucaria*. There are two possible future scenarios for these crystallites: they can move to the outer side of the basal wall and remain as wedge-shaped crystallites (Fig. 5C, D), or they can remain on the inner surface and transform into foliated crystallites. The crystallites that remain on the inner side gradually became more structured. At the same time, their growth became more organized, as evidenced by the growth lines of crystallites of different ages, particularly foliated (Fig. 6E). Crystallites that moved to the outer side of the basal wall stopped growing and were covered by the cuticle. Based on these findings, the pattern of skeletal growth in *P. verrucaria* can be described as follows: first, at the distal ends of the colony, the epithelial cells of the basal wall secrete a cuticle. Crystallites are then deposited on the cuticle and gradually increase in size as a result of ongoing, orderly secretion of calcium carbonate onto the existing crystallites. Simultaneously, additional crystallites continued to form at the growing edge. The growing edge of the colony advances at a relatively constant rate, which can be determined from the approximately equal spacing between the growth lines on the foliated crystallites and the constant width of the accretion zone. The process of skeletal formation in cyclostome bryozoans is similar to that in bivalves (Clark *et al.*, 2020). Our data also confirm that skeletal formation is carried out due to direct contact of the epithelium with crystallites, as it was demonstrated earlier for other representatives of the Cyclostomatida (Grenier *et al.*, 2023, 2024). This is an important difference between cyclostomes and cheilostome bryozoans, in which skeletal formation occurs mainly without epithelial contact with crystallites (Grenier *et al.*, 2024).

The presence of a granular fabric may be an indicator of colony growth at a particular location. For example, it is evident that a growth zone is formed during the development of the brood chamber in the Lichenoporidae family. It is believed that this structure is formed as a result of the accumulation of alveoli and their subsequent absorption into its walls. The wedge-shaped and intermediate crystallites extending from the alveolar walls towards the centre may also be further evidence of this formation process. In addition, any deviation in the skeletal structure within the brood chamber compared to the typical structure may indicate skeletal disintegration.

The ordered growth lines on crystallites, the pustules arranged in a certain order, and the several skeletal growth zones inside the colony indicate that cyclostome bryozoans are active biomineralizers. In this regard, they must have the special biochemical structures responsible for this process. In addition, the enzyme complex involved in the mineralization must be able to correctly orient individual atoms, since the skeleton of Cyclostomatida consists exclusively

of the calcite form of calcium carbonate. Understanding the structure of this apparatus and the mechanism of skeletal secretion may be the key to creating new materials, as it was suggested for Bivalvia (Clark *et al.*, 2020). However, unlike bivalves (Weiner, Traub, 1984; Marin *et al.*, 2005; Zhang *et al.*, 2006; Fang *et al.*, 2011; Clark *et al.*, 2020; Yarra *et al.*, 2021), there are few studies in this area for bryozoans so far (Achilleos *et al.*, 2024). Due to its abundance (for example, in the White Sea) and some structural features, *P. verrucaria* is a promising object for research in this area. In addition to the growing edge and the rest of the colony, where biomineralization is less active, this species has a zone in which a brood chamber is formed. Thus, it is possible to determine whether this mechanism is uniform across all the biomineralization sites.

Congruence with molecular phylogeny

The microstructure of the cyclostome skeleton was described in detail in a series of publications by Taylor and co-authors (Taylor, Jones, 1993; Taylor *et al.*, 1995; Weedon, Taylor, 1996, 1997, 1998; Taylor, Weedon, 2000). They described six main microstructural fabrics in cyclostomes differing in their crystallite orientation, shape, and prevailing growth directions: granular, planar spherulitic, transverse fibrous, foliaceous, rhombic semi-nacreous, hexagonal semi-nacreous (and pseudofoliated) (Taylor, Weedon, 2000). In the suborders of cyclostome bryozoans, five different fabric suits are observed in the inner walls (hereinafter referred to as IFS, or inner fabric suits, and they are presented in Tab. 1). All walls of *P. verrucaria*, with the exception of the basal one, are inner (covered on all sides by epithelial tissue) and as mentioned above, consist of two fabrics (granular and foliated). This wall structure belongs to the second type of fabric suits (Tab.1) and is characteristic mainly of representatives of two suborders Rectangulata and some "Cerioporina". It should also be noted that IFS-2 and IFS-3 are similar and differ in the type of mature fabric: foliated or hexagonal semi-nacreous. At the same time, hexagonal semi-nacreous suit is a modified version of foliated fabric (Taylor, Weedon, 2000). Therefore, IFS-3 is likely a modification of IFS-2. IFS-3 is also observed in some representatives of tubuliporines, along with IFS-1,4,5.

Based on cladistic analysis by Taylor and Weedon (2000), microstructural features were considered to have the most homoplasic. Furthermore, microstructural characters in cyclostome bryozoans appear to be more prone to homoplasy than zooidal and colonial characters. This suggests that the use of microstructural characters as a basis for systematic classification of these organisms may be challenging. However, it is possible that this situation is more complex than initially thought.

Mapping of fabric suits on phylogenetic trees (Waeschenbach *et al.*, 2009, Taylor *et al.*, 2021) obtained using molecular biology techniques, revealed that IFS-4 is a derived characteristic of the family Crisiidae. However, studied species from the family Crisuliporidae do not form a monophyletic group with the Crisiidae, and instead, IFS-4 possess IFS-1. Therefore, IFS-4 can be considered an apomorphic trait of the suborder Articulata, excluding the Crisuliporidae family.

Studies using molecular biology techniques have revealed that representatives of the families Rectangulata (which have IFS-2), Densiporidae (possessing IFS-2) and some members of Plagioeciidae (having IFS-3), form a monophyletic group with the representatives of Rectangulata (group A). It is worth noting that IFS-2 and IFS-3 are found in a larger number of Cyclostomatida, although molecular data are lacking for most of these bryozoans. Some species having IFS-3, including *Diplosolen obelium* and *Cardioecia watersi*, are significantly distant from the aforementioned group; however, they form a distinct clade (group B). It is possible that there are structural or developmental differences among bryozoans with IFS-3 belonging to these two separate groups that were not considered in previous studies. For instance, "Blue disporella" (having IFS-2) exhibits screw dislocations characteristic of hexagonal semi-nacreous fabric, as seen in IFS-3, and the broad, foliated crystallites of *P. radiata* are similar to the pseudofoliated crystallites found in *Plagioecia dorsalis*.

For the clade A, consisting of representatives of the genera *Plagioecia* (Tubuliporina), *Favosipora* (Cerioporina), *Doliocoitis* (Rectangulata), and *Disporella* (Rectangulata), a putative microstructural character ("...absence of semi-nacre/pseudofoliated fabric in the skeleton...") has been proposed (Taylor *et al.*, 2021). However, this hypothesis contradicts the data of Taylor and Weedon (Weedon, Taylor, 1997; Taylor, Weedon, 2000), who indicate the presence of hexagonal seminacres in representatives of the genus *Plagioecia*. A putative character for these

Table 1. Presence of the different fabric suits among Cyclostomatida suborders.

	Rectangulata (Taylor, Weedon, 2000)	"Tubuliporine" (Taylor, Weedon, 2000)	"Cerioporine" (Taylor, Weedon, 2000)	"Articulata" (Taylor, Weedon, 2000)	"Cancellates" (Taylor, Weedon, 2000)	*Patinella verrucaria* (recent study)
IFS-1 (PS + TF + F + HS)		+ (*Tubulipora*, *Cinctipora* etc.)	+ (*Heteropora neozelanica*, *H. parapellirulata*)	+ (*Crisulipora*)	+ (*Siphodictyum gracile* – fossil)	
IFS-2 (G+F)	+ (e.g. *Disporella*, *Patinella radiata*)	+ (*Idmidronea obtecta*)	+ (*Heteropora*, *Densipora*, *Favosipora*)			+
IFS-3 (G+HS)		+ (*Plagioecia*, *Diplosolen obelia*, *Cardioeca* etc.)				
IFS-4 (HS+DPf)		+ ("*Stomatopora*")		+(*Bicrisia*, *Crisia*)	+ (all apart *H. squamosa*)	
IFS-5 (HS+PPf)		*Fenestulipora*			+ (*Hornera*, *Crisina*)	

Abbreviations: IFS 1–5 — interior wall fabric suits, PS — planar spherulitic fabric, TF — transverse fibrous, F — foliated, HS — hexagonal semi-nacre, G — granular, DPf — distally-imbricated pseudofoliated, PPf — proximally-imbricated pseudofoliated.

two clades could be the presence of both IFS-2 and IFS-3, assuming that there are structural or developmental differences in IFS-3 between clade A and clade B.

Taylor and Weedon (2000) proposed that the high degree of homoplasy in microstructural features can be due to the fact that genera were identified based on colonial characteristics. Had cyclostome genera been defined on the basis of ultrastructural characters, the results may have been the opposite.

From the above, it follows that the IFS can serve as an important defining character for some groups at the family and suborder levels. Furthermore, these and previous analyses did not consider data on the appearance of fabric suits, which may be useful for phylogenetic analyses. Moreover, molecular data on Cyclostomatida species are extremely limited (Waeschenbach *et al.*, 2009; Taylor *et al.*, 2011, 2015, 2021). Therefore, further studies aimed at examining the microstructure of their skeletons and comparing them with molecular biological data could help better understand the relationships between families, the evolutionary history of this group, and clarify its taxonomy.

Comparison within Lichenoporidae

Our data has shown that *P. verrucaria* has following microstructure characteristics: type 2 microstructure fabric, width of foliated crystallites is 5–20 μm, numerous pustules in interior walls forming at growth margin, absence of mural spines and 1–3 apertural spines (Tab. 2). According to this, the crystallites of *P. verrucaria* are more similar linear dimensions to those of *Disporella gordoni* and "blue Disporella" (Taylor *et al*., 1995) than to *Patinella* (*Lichenopora*) *radiata* (Taylor *et al.*, 1995) (Tab. 2). A similar condition of pustules was reported for *D. gordoni* (Taylor *et al*., 1995) and unidentified *Patinella* sp. (Ramalho *et al.*, 2009) (Tab. 2). In addition to pustules, *P. radiata*, *D. gordoni* and *Patinella* sp. possess mural spines; the latter are absent in *P. verrucaria* and *D. gordoni*. The number of apertural spines in studies species is variable: *P. verrucaria* has 1–3 spines, while *Patinella*

Table 2. Microstructural and sculptural features of some Lichenoporidae species. Note differences in wide of foliaceous crystallites and the presence/absence of the pustules.

	Patinella verrucaria (recent study)	*Patinella radiata* (Taylor *et al*., 1995)	*Patinella* sp. (Ramalho *et al*., 2009)	"Blue Disporella" (Taylor *et al*., 1995)	*Disporella gordoni* (Taylor *et al*., 1995)
Number of apertural spines	1–3	N/D	8–10	2	1
Wide of foliated crystallites (μm)	5–20	up to 100	N/D	5–25	5–25
Fabrics in interior walls	granular foliated	granular foliated	N/D	granular foliated	granular foliated
Microstructure fabric of the interior walls	type 2	type 2	N/D	type 2	type 2
Mural spines	absent	thorn-like	straight or slightly curved	thorn-like	absent
Size of the mural spines	absent	up to 30 μm long and 5–10 μm in diameter	up to 30 μm long	up to 30 pm long and 5–10 pm in diameter	absent
Place of pustule formation	growth margin	absent	growth margin	N/D	growth margin
Arrangement of newly formed pustules	in rows	absent	N/D	N/D	N/D
Number of pustules	numerous	absent	numerous	N/D	numerous
Height of Pustules (max in μm)	10–12	absent	N/D	N/D	N/D

Abbreviations: N/D — no data.

sp. has 6–8. Hence, the microstructure and micro- and macrosculpture demonstrate a mosaic distribution at both the genus and species levels.

Pustules

Special attention should be paid to pustules, which are needle-like microstructures. In *P. verrucaria*, pustules are located on the inner side of the basal wall, interzooidal walls, and brood chamber; they reach 12 μm in height. Similar structures have been observed in other species of this family, but their exact function remains unclear (Taylor *et al.*, 1995). Thus, the brood chambers of *Disporella hispida* are particularly rich in pustules. If there are several ooeciostomes, they differ in the arrangement of the pustules: one ooeciostome bears them close to the aperture, while the others they are located deeper. Functional ooeciostomes should contain "upper cell complex" (our unpublished data and a similar complex is also formed in the gonozooids of Crisiidae (Nekliudova *et al.*, 2021))

The cells of this complex can use pustules for attachment. Thus, we suggest, that the only functional ooeciostome bears pustules close to the aperture. Also, these pustules perform a similar function in other parts of the colony, helping to elevate the epithelium and facilitate fluid transport within the colony. Therefore, pustules perform a structural function. A similar function is assumed for the acanthostyles of extinct representatives of Stenolaemata (Ernst, 2020), which may have performed the same structural functions as pustules, but also a protective one.

Are the alveoli still kenozooids?

In a lichenoporid colony, there are autozooids, brood chambers, and alveoli. Alveoli are interzooidal spaces between the autozooecia in rectangulate cyclostomes, which are enclosed

by calcified interior wall (Pitt, Taylor, 1990). The nature of the alveoli is still debated: some authors (Gordon, Taylor, 2001; Taylor, Grischenko, 2015; Taylor *et al.*, 2021) consider them kenozooids, while others (Harmer, 1896; Borg, 1926; Gostilovskaya, 1978; Alvarez, 1995; Ramalho *et al.*, 2009) do not. A kenozooid is a heterozooid without a polypide, usually without an orifice or muscles (glossary bryozoa.net). In the case of Lichenoporidae, the two terms largely coincide, as polypides, muscles, and openings are absent in the alveoli of *P. verrucaria* or other members of this family. Instead, they are lined with epithelium, and their walls also contain pores. The pores connecting the alveoli to each other or to the autozuoids are similar in structure and size to the pores between the autozuoids and on the roof of the brood chamber. The formation of alveoli on the growing edge of the colony follows the same pattern as in autozooids, and the secondary alveoli forming on the roof of the adult brood chamber are also connected to it by pores. Similar "cells", known as kenozooids, are found in other families, such as Densiporidae, including *Favosipora* (Gordon, Taylor, 2001). These "cells" appear to play an important structural role in the arrangement of autozooids within the colony and facilitate the development of the brood chamber in both families.

The similarity in the formation of alveoli and autozooids in *P. verrucaria*, as well as the presence of pores and functionality similar to kenozooids in Densiporidae, suggests that the term "kenozooids" is more appropriate for these structures. The term "alveoli", which describes these "cells", should be abandoned. In addition, the presence of kenozooids with similar structure in representatives of Lichenoporidae and some Densiporidae is in a good agreement with the molecular data, indicating a close phylogenetic relationship between the genera *Disporella*, *Patinella* (unpublished data), and *Favosipora*.

Conclusion

A study of the skeleton of *Patinella verrucaria* using modern methods has revealed several important features.

We confirm the presence of two variants of early astogeny in *P. verrucaria*, which can be attributed to both genetic predisposition and external factors, primarily mechanical stress. Regardless of the cause, the features of early colony development can be used for phylogenetic analysis, although further studies of other representatives of this order are needed. In addition, these two developmental pathways represent an excellent opportunity to study the evolution of colonial organisms.

IFS appears to be heterogeneously distributed among Cyclostomatida. Nevertheless, in some families this microstructural feature acts as an apomorphic character. Further studies using SEM and molecular methods are required for a more confident application of the wall structure features.

Fabric suit of *P. verrucaria* is similar to that of other representatives of the Lichenoporidae. However, there are some differences in the fine structure between the species in the family. These differences at the microstructural level can be used to identify species within the family.

The skeletal formation of *P. verrucaria* is similar to that observed in other cyclostomes and resembles that of Mollusca. The abundance of this species in the White Sea, as well as the presence of zones of active and inactive skeletal development, allow us to suggest *P. verrucaria* as a potential model organism for studying the biochemical processes involved in skeletal formation. Understanding these processes may be important for the development of new materials.

Pustules appear to support and elevate the epithelium, facilitating the transport of substances within the colony.

The microstructure of the alveoli and their similarity in structure and function to the kenozooids of *Favosipora* suggest that it is more appropriate to term them kenozooids.

Compliance with ethical standards.

CONFLICTS OF INTEREST: The authors declare no competing of interests.

Acknowledgments. The authors are thankful to the management and staff of Pertsov White Sea Biological Station of Lomonosov Moscow State University (WSBS MSU) for providing the opportunity to conduct the research and especially to WSBS diving team. We are also thankful to the centre of electron microscopy of MSU and computed microtomograph operators. Special thanks to our colleague K.G. Kotova for her help in identifying the types of colony development. The work of ENT is supported by Russian Science Foundation (No. 23-14-00020).

References

Achilleos K., Smith A.M., Kenny N.J., Brown C.M. 2024. A new transcriptome resource for *Cellaria immersa* (Phylum: Bryozoa) reveals candidate genes and proteins related to biomineralization // Frontiers in Marine Science. Vol.11. Art.1389708.

Batson P.B., Taylor P.D., Smith A.M. 2019. Early astogeny in'Hornera'(Bryozoa; Cyclostomata; Cancellata) // Australasian Palaeontological Memoirs. Vol.52. P.23–30.

Blake D.B. 1980. Homeomorphy in Paleozoic bryozoans: a search for explanations // Paleobiology. Vol.6. No.4. P.451– 465.

Blum M., Ott T. 2018. Animal left–right asymmetry // Current Biology. Vol.28. No.7. P.R301–R304.

Boardman R.S. 1998. Reflections on the morphology, anatomy, evolution, and classification of the class Stenolaemata (Bryozoa) // Smithsonian contributions to paleobiology. No.86. P.1–60.

Boardman R.S., McKinney F.K., Taylor P.D. 1992. Morphology, anatomy, and systematics of the Cinctiporidae, new family (Bryozoa: Stenolaemata) // Smithsonian contributions to paleobiology. No.70. P.1–81.

Borg F. 1926. Studies on recent cyclostomatous Bryozoa. 499 p.

Brood K. 1976. Wall structure and evolution in cyclostomate Bryozoa // Lethaia. Vol.9. No.4. P.377–389.

Clark M.S., Peck L.S., Arivalagan J., Backeljau T., Berland S., Cardoso J.C.R., Caurcel C., Chapelle G., De Noia M., Dupont S., Gharbi K., Hoffman J.I., Last K.S., Marie A., Melzner F., Michalek K., Morris J., Power D.M., Ramesh K., Sanders T., Sillanpää K., Sleight V.A., Stewart-Sinclair P.J., Sundell K., Telesca L., Vendrami D.L.J., Ventura A., Wilding T.A., Yarra T., Harper E.M. 2020. Deciphering mollusc shell production: the roles of genetic mechanisms through to ecology, aquaculture and biomimetics // Biological Reviews. Vol.95. No.6. P.1812–1837.

Demidova M., Vishnyakov A., Karagodina N., Kotenko O., Nekliudova U., Bogdanov E., Ostrovsky A. 2025. Vertical transfer of bacterial symbionts via a placental analogue in the cyclostome bryozoan *Patinella verrrucaria* (Stenolaemata): ultrastructural and molecular evidence // Zoology. Vol.171. Art.126281.

Denley D., Metaxas A., Short J. 2014. Selective settlement by larvae of *Membranipora membranacea* and *Electra pilosa* (Ectoprocta) along kelp blades in Nova Scotia, Canada // Aquatic Biology. Vol.21. No.1. P.47–56.

Ernst A. 2017. Diversity dynamics of Ordovician Bryozoa // Lethaia. Vol.51. No.2. P.198–206.

Ernst A. 2020. Fossil record and evolution of Bryozoa // Phylum Bryozoa. P.11–55.

Ernst A., Jackson P.N.W., Aretz M. 2015. Bryozoan fauna from the Mississippian (Visean) of Roque Redonde (Montagne Noire, southern France) // Geodiversitas. Vol.37. No.2. P.151–213.

Fang D., Xu G., Hu Y., Pan C., Xie L., Zhang R. 2011. Identification of Genes Directly Involved in Shell Formation and Their Functions in Pearl Oyster, Pinctada fucata // PLOS ONE. Vol.6. No.7. Art.e21860.

Freeman G., Lundelius J.W. 1982. The developmental genetics of dextrality and sinistrality in the gastropodLymnaea peregra // Wilhelm Roux's archives of developmental biology. Vol.191. No.2. P.69–83.

Glossary at bryozoa. net Online at https://www.bryozoa.net/glossary.html

Gostilovskaya M.G. 1978. [Identifier of the White Sea bryozoans]. Leningrad: Nauka Publ, Leningrad Dept. 248 p. [In Russian]

Gordon D., Taylor P. 2001. New Zealand Recent Densiporidae and Lichenoporidae (Bryozoa: Cyclostomata) // Species Diversity. Vol.6. P.243–290.

Gould S.J., Young N.D., Kasson B. 1985. The consequences of being different: sinistral coiling in Cerion // Evolution. Vol.39. P.1364–1379.

Govind C.K. 1989. Asymmetry in Lobster Claws // American Scientist. Vol.77. No.5. P.468–474.

Grenier C., Griesshaber E., Schmahl W., Berning B., Checa A.G. 2024. Skeletal microstructures of cheilostome bryozoans (phylum Bryozoa, class Gymnolaemata): crystallography and secretion patterns // Marine Life Science & Technology. Vol.6. No.3. P.405–424.

Grenier C., Griesshaber E., Schmahl W.W., Checa A.G. 2023. Microstructure and crystallographic characteristics of stenolaemate bryozoans (phylum Bryozoa and class Stenolaemata) // Crystal Growth & Design. Vol.23. No.2. P.965–979.

Harmer S.F. 1896. On the development of *Lichenopora verrucaria*, Fabr. // Journal of Cell Science. Vol.2. P.71–144.

Hinds R.W. 1975. Growth Mode and Homeomorphism in Cyclostome Bryozoa // Journal of Paleontology. Vol.49. No.5. P.875–910.

Ma J., Taylor P.D., Xia F., Zhan R. 2015. The oldest known bryozoan: *Prophyllodictya* (Cryptostomata) from the lower Tremadocian (Lower Ordovician) of Liujiachang, south-western Hubei, central China // Palaeontology. Vol.58. No.5. P.925–934.

Marin F., Amons R., Guichard N., Stigter M., Hecker A., Luquet G., Layrolle P., Alcaraz G., Riondet C., Westbroek P. 2005. Caspartin and Calprismin, Two Proteins of the Shell Calcitic Prisms of the Mediterranean Fan Mussel *Pinna nobilis* // Journal of Biological Chemistry. Vol.280. No.40. P.33895–33908.

McKinney F. 1998. Avicularia-like structures in a Paleozoic fenestrate bryozoan // Journal of Paleontology. Vol.72. No.5. P.819–826.

McKinney F.K., McKinney M.J. 1993. Larval behaviour and choice of settlement site: Correlation with environmental distribution pattern in an erect bryozoan // Facies. Vol.29. No.1. P.119–131.

Medd A. 1966. The zoarial development of some membranimorph Polyzoa // Annals and Magazine of Natural History. Vol.9. Is.97–99. P.11–22.

Nekliudova U., Schwaha T., Kotenko O., Gruber D., Cyran N., Ostrovsky A. 2021. Three in one: evolution of viviparity, coenocytic placenta and polyembryony in cyclostome bryozoans // BMC Ecology and Evolution. Vol.21. No.1. P.1–34.

Nielsen C. 1970. On metamorphosis and ancestrula formation in cyclostomatous bryozoans // Ophelia. Vol.7. No.2. P.217–256.

Nielsen C., Bekkouche N.T., Worsaae K. 2019. Neuromuscular structure of the larva to early ancestrula stages of the cyclostome bryozoan *Crisia eburnea* // Acta Zoologica. Vol.100. No.3. P.268–281.

Nielsen C., Pedersen K.J. 1979. Cystid structure and protrusion of the polypide in *Crisia* (Bryozoa, Cyclostomata) // Acta Zoologica. Vol.60. No.2. P.65–88.

Palmer A.R. 1996. From symmetry to asymmetry: phylogenetic patterns of asymmetry variation in animals and their evolutionary significance // Proceedings of the National Academy of Sciences. Vol.93. No.25. P.14279–14286.

Palmer A.R. 2009. Animal asymmetry // Current Biology. Vol.19. No.12. P.R473–R477.

Pitt L., Taylor P. 1990. Cretaceous Bryozoa from the Faringdon Sponge Gravel (Aptian) of Oxfordshire // Bulletin of the British Museum, Natural History. Geology. Vol.46. No.1. P.61–152.

Pruss S., Leeser L., Smith E., Zhuravlev A., Taylor P. 2022. The oldest mineralized bryozoan? A possible palaeostomate in the lower Cambrian of Nevada, USA // Science Advances. Vol.8. No.16. Art.8465.

Roberts D., Rittschof D., Holm E., Schmidt A.R. 1991. Factors influencing initial larval settlement: temporal, spatial and surface molecular components // Journal of Experimental Marine Biology and Ecology. Vol.150. No.2. P.203–221.

Schäfer P. 1991. Brutkammern der Stenolaemata (Bryozoa): Konstruktionsmorphologie und phylogenetische Bedeutung. 262 S.

Schwaha T.F., Handschuh S., Ostrovsky A.N., Wanninger A. 2018. Morphology of the bryozoan *Cinctipora elegans* (Cyclostomata, Cinctiporidae) with first data on its sexual reproduction and the cyclostome neuro-muscular system // BMC Evolutionary Biology. Vol.18. No.1. P.18–92.

Snijder E.A. 2024. Investigating abiotic and biotic factors related to the growth of bryozoans on kelp lamina. MS thesis NTNU.

Tamberg Y., Batson P., Napper R. 2021. Polypide anatomy of hornerid bryozoans (Stenolaemata: Cyclostomatida) // Journal of Morphology. Vol.282. No.11. P.1708–1725.

Tamberg Y., Batson P.B., Smith A.M. 2022. The epithelial layers of the body wall in hornerid bryozoans (Stenolaemata: Cyclostomatida) // Journal of Morphology. Vol.283. No.4. P.406–427.

Tavener-Smith R., Williams A. 1972. The secretion and structure of the skeleton of living and fossil Bryozoa // Philosophical Transactions of the Royal Society of London. B, Biological Sciences. Vol.264. No.859. P.97–160.

Taylor P. 1994. An early cheilosteme bryozoan from the Upper Jurassic oy Yemen // Neues Jahrbuch für Geologie und Paläontologie-Abhandlungen. Vol.191. No.3. P.331–344.

Taylor P.D., Grischenko A.V. 2015. Two new species of heavily calcified cyclostome bryozoans from the intertidal of Akkeshi Bay, Hokkaido, Japan // Journal of Natural History. Vol.49. No.29–30. P.1763–1775.

Taylor P.D., Harmelin J.-G., Waeschenbach A., Bouchon C. 2021. *Disporella guada* sp. nov., an erect-ramose rectangulate cyclostome (Bryozoa, Stenolaemata) from the Caribbean Sea: convergent evolution in bryozoan colony morphology // European Journal of Taxonomy. Vol.773. P.1–18.

Taylor P.D., Jones C.G. 1993. Skeletal Ultrastructure in the Cyclostome Bryozoan Hornera // Acta Zoologica. Vol.74. No.2. P.135–143.

Taylor P.D., Waeschenbach A., Florence W. 2011. Phylogenetic position and systematics of the bryozoan *Tennysonia*: further evidence for convergence and plasticity in skeletal morphology among cyclostome bryozoans // Zootaxa. Vol.3010. No.1. P.58–68.

Taylor P.D., Waeschenbach A., Smith A.M., Gordon D.P. 2015. In search of phylogenetic congruence between molecular and morphological data in bryozoans with extreme adult skeletal heteromorphy // Systematics and Biodiversity. Vol.13. No.6. P.525–544.

Taylor P.D., Weedon M.J. 2000. Skeletal ultrastructure and phylogeny of cyclostome bryozoans // Zoological Journal of the Linnean Society. Vol.128. No.4. P.337–399.

Taylor P.D., Weedon M.J., Jones C.G. 1995. Skeletal Ultrastructure in some Cyclostome Bryozoans of the Family Lichenoporidae // Acta Zoologica. Vol.76. No.3. P.205–216.

Temereva E.N., Kosevich I.A. 2018. The nervous system in the cyclostome bryozoan *Crisia eburnea* as revealed by transmission electron and confocal laser scanning microscopy // Frontiers in zoology. Vol.15. No.1. P.1–15.

Viskova L.A. 2013. [Phenomenon of enantiomorphisms in bryozoans] // Simmetriya i asimmetriya. P.145–164 [in Russian].

Viskova L. 2014. Phenomenon of enantiomorphism in marine bryozoans // Paleontological Journal. Vol.48. No.11. P.1194–1206.

Waeschenbach A., Cox C.J., Littlewood D.T.J., Porter J.S., Taylor P.D. 2009. First molecular estimate of cyclostome bryozoan phylogeny confirms extensive homoplasy among skeletal characters used in traditional taxonomy // Molecular Phylogenetics and Evolution. Vol.52. No.1. P.241–251.

Weedon M.J., Taylor P.D. 1995. Calcitic Nacreous Ultrastructures in Bryozoans: Implications for Comparative Biomineralization of Lophophorates and Molluscs // The Biological bulletin. Vol.188. No.3. P.281–292.

Weedon M.J., Taylor P.D. 1996. Skeletal Ultrastructures in some Cerioporine Cyclostome Bryozoans // Acta Zoologica. Vol.77. No.3. P.249–265.

Weedon M.J., Taylor P.D. 1997. Skeletal Ultrastructure in some Tubuliporine Cyclostome Bryozoans // Acta Zoologica. Vol.78. No.2. P.107–121.

Weedon M.J., Taylor P.D. 1998. Skeletal Ultrastructure in Some Articulate Cyclostome Bryozoans // Acta Zoologica. Vol.79. No.2. P.133–148.

Weiner S., Traub W. 1984. Macromolecules in mollusc shells and their functions in biomineralization // Philosophical Transactions of the Royal Society of London. B, Biological Sciences. Vol.304. No.1121. P.425–434.

Worsaae K., Frykman T., Nielsen C. 2020. The neuromuscular system of the cyclostome bryozoan *Crisia eburnea* (Linnaeus, 1758) // Acta Zoologica. Vol.101. No.2. P.133–146.

Yagunova E. 2005. [Astogeny of the *Cribrillina annulata* (Fabricus, 1780) (Bryozoa: Cheilostomata): norm and anomaly] // Invertebrate Zoology. Vol.2. No.2. P.203–216 [in Russian].

Yarra T., Blaxter M., Clark M.S. 2021. A Bivalve Biomineralization Toolbox // Molecular Biology and Evolution. Vol.38. No.9. P.4043-4055.

Zhang C., Li S., Ma Z., Xie L., Zhang R. 2006. A Novel Matrix Protein p10 from the Nacre of Pearl Oyster (Pinctada fucata) and Its Effects on Both CaCO3 Crystal Formation and Mineralogenic Cells // Marine Biotechnology. Vol.8. No.6. P.624-633.

Responsible editor A.I. Granovich